

Journal of Mechanics of Materials and Structures

**PATH-INDEPENDENT H-INTEGRAL FOR INTERFACE CORNERS UNDER
THERMAL LOADINGS**

Chyanbin Hwu, Tai-Liang Kuo and Chun-Chih Huang

Volume 6, No. 1-4

January–June 2011

PATH-INDEPENDENT H-INTEGRAL FOR INTERFACE CORNERS UNDER THERMAL LOADINGS

CHYANBIN HWU, TAI-LIANG KUO AND CHUN-CHIH HUANG

It is well known that the path-independent H-integral is an appropriate tool for calculating the mixed mode stress intensity factors for the interface corners between dissimilar elastic materials. To extend the applicability of the H-integral from the mechanical loading condition to the thermal loading condition, a modified H-integral is proposed in this paper. This modified H-integral possesses an extra domain integral which needs the input of temperature field. Moreover, this domain integral contains singular functions that come from the strain components of the auxiliary system, and a special treatment should be made for the accurate computation of stress intensity factors. The near-tip solutions and auxiliary solutions of displacements, stresses, and temperature required in the calculation of H-integral are all provided in this paper. The validity and versatility of the proposed approach are then shown by carrying out several numerical examples such as cracks under mixed-mode thermal loadings, interface cracks/corners under uniform heat flow or uniform temperature change, and an electronic package, in which the chip has a heat generation rate, placed at a constant temperature ambience.

1. Introduction

Many engineering objects, for example electronic packages, engines of power vehicles, solar panels, and so on, are operated in thermal environments. Temperature changes, heat flux on the object surface, and heat generation in the interior can deform the object and induce stress when restrictions on deformation are imposed, such as a clamped boundary condition or a perfect-bonded condition along an interface between dissimilar materials. Interface corners commonly appear in these engineering objects and failures initiate from these critical regions due to discontinuities of geometry and material properties. Hence, methods of fracture analysis for estimating the potential of failure and the mode of fracture of interface corners in elastic materials subjected to thermal loading are of great importance. Orders of stress singularity and stress intensity factors are two commonly used parameters when we perform fracture analyses within the category of linear elastic fracture mechanics.

This paper provides an accurate, efficient, and systematic solution technique to calculate these two parameters for interface corners between dissimilar elastic materials subjected to thermal loading.

Studies of fracture analysis of interface cracks subjected to thermal loadings include [Erdogan 1965; Brown and Erdogan 1968; Hwu 1990; 1992; Ikeda and Sun 2001; Banks-Sills and Dolev 2004; Nagai et al. 2007]. Relatively few studies have dealt with interface corners; they include [Munz and Yang 1992; 1993; Banks-Sills and Ishbir 2004; Hwu and Lee 2004; Nomura et al. 2009]. To understand the

The authors thank the National Science Council, Taiwan, for support through Grant NSC 98-2221-E-006-121-MY3.

Keywords: interface corner, order of stress singularity, order of heat flux singularity, stress intensity factor, Stroh formalism, thermoelasticity.

mechanical behavior of anisotropic elastic materials under thermal environments, Stroh formalism [Stroh 1958; Ting 1996; Hwu 2010] for two-dimensional linear anisotropic thermoelasticity has been employed in many works [Clements 1973; Hwu 1990]. By this formalism, analytical closed-form solutions for the orders of heat flux/stress singularity and near-tip solutions of multimaterial anisotropic wedges under thermal loadings have been obtained in [Hwu and Lee 2004]. To understand the fracture behavior of interface corners, a unified definition of stress intensity factors for connecting cracks, corners, interface cracks, and interface corners was proposed in [Hwu and Kuo 2007]. In that work, in order to avoid the oscillatory singular problems of interface corners a path-independent H-integral [Bueckner 1973; Stern 1976] was suggested to calculate the stress intensity factors. Based on these works, in this paper the H-integral is further modified to be suitable for the thermal loading condition.

The modified H-integral contains an additional domain integral that is not included in the H-integral for pure mechanical loading. The integrand in this domain integral contains singular functions that come from the strain components in the auxiliary system. Considerable numerical error will be induced if we perform this domain integral via normal numerical methods, for example, Simpson's rule and Gaussian quadrature. To deal with this problem, the domain integral is separated into two parts. One is the near-tip part, to be integrated analytically, and the other is the adjacent part, to be calculated numerically. A similar approach has been proposed by [Banks-Sills and Ishbir 2004; Nomura et al. 2009].

Several numerical examples are analyzed for the purpose of verification: a center crack under mixed-mode thermal loading, a center interface crack under uniform heat flow, edge interface cracks under uniform temperature change, and interface corners under uniform temperature change. In addition, an example about electronic packages is analyzed to show the feasibility and practicability of the modified H-integral.

2. Thermoelastic analysis of interface corners

In a fixed rectangular coordinate system x_i , $i = 1, 2, 3$, let u_i , σ_{ij} , ϵ_{ij} , T , and h_i be, respectively, the displacement, stress, strain, temperature, and heat flux. The heat conduction, energy equation, strain-displacement relation, constitutive law, and equilibrium equations for the uncoupled steady state thermoelastic problems can be written as [Nowacki 1962]

$$h_i = -k_{ij}T_{,j}, \quad h_{i,i} = 0, \quad \epsilon_{ij} = \frac{1}{2}(u_{i,j} + u_{j,i}), \quad \sigma_{ij} = C_{ijks}\epsilon_{ks} - \beta_{ij}T, \quad \sigma_{ij,j} = 0, \quad i, j, k, s = 1, 2, 3, \quad (1)$$

where repeated indices imply summation, a comma stands for differentiation, and C_{ijks} , k_{ij} , and β_{ij} are, respectively, the elastic constants, heat conduction coefficients, and thermal moduli. C_{ijks} are assumed to be fully symmetric, that is, $C_{ijks} = C_{jiks} = C_{ijsk} = C_{ksij}$, and are required to be positive definite due to the positiveness of the strain energy. β_{ij} and k_{ij} are also assumed to be symmetric, that is, $\beta_{ij} = \beta_{ji}$ and $k_{ij} = k_{ji}$.

Consider an interface corner between two dissimilar anisotropic elastic materials (Figure 1) in which a local polar coordinate system (r, θ) is specified at the corner tip. Assume a perfect bond along the interface. The displacement, traction, temperature, and heat flux continuity across the interface $\theta = 0$ can be written as [Hwu and Lee 2004]

$$\mathbf{u}_1(0) = \mathbf{u}_2(0), \quad \boldsymbol{\phi}_1(0) = \boldsymbol{\phi}_2(0), \quad T_1(0) = T_2(0), \quad h_1^*(0) = h_2^*(0), \quad (2a)$$

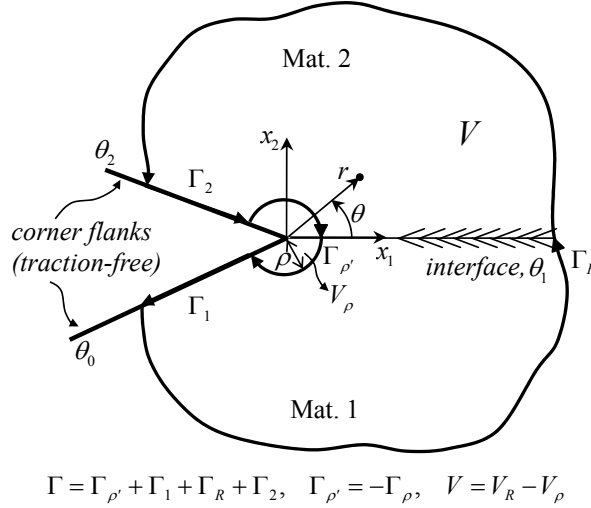


Figure 1. A closed contour Γ and its domain V for the H-integral of an interface corner.

where \mathbf{u} and $\boldsymbol{\phi}$ are, respectively, the displacement vector and stress function vector; h^* is the heat flux in the direction normal to the interface; the subscripts 1 and 2 stand for the values related to materials 1 and 2; and the argument 0 denotes the value on the interface. The corner flanks are both assumed to be traction-free which can be expressed by the stress function as

$$\boldsymbol{\phi}_1(\theta_0) = \boldsymbol{\phi}_2(\theta_2) = \mathbf{0}. \tag{2b}$$

Four different thermal conditions on the corner flanks are considered in this paper:

$$\begin{aligned} \text{isothermal-isothermal: } & T_{1,r}(\theta_0) = T_{2,r}(\theta_2) = 0, \\ \text{insulated-insulated: } & h_1^*(\theta_0) = h_2^*(\theta_2) = 0, \\ \text{insulated-isothermal: } & h_1^*(\theta_0) = T_{2,r}(\theta_2) = 0, \\ \text{isothermal-insulated: } & T_{1,r}(\theta_0) = h_2^*(\theta_2) = 0. \end{aligned} \tag{2c}$$

Note that the components of stress function vector, $\phi_i, i = 1, 2, 3$, are related to the stresses σ_{ij} and the surface traction t_i by

$$\sigma_{i1} = -\phi_{i,2}, \quad \sigma_{i2} = \phi_{i,1}, \quad t_i = \sigma_{ij}n_j = \frac{d\phi_i}{ds}, \tag{3}$$

where n_i is the normal of the surface and s is the tangential.

3. Near-tip solutions

The near-tip solutions satisfying all the basic equations (1) and boundary conditions (2) were obtained in our previous study [Hwu and Lee 2004] as

$$\mathbf{v}(r, \theta) = -\delta(1 - \delta)r^{-1-\delta}\mathbf{\Gamma}(\theta)\mathbf{v}_0, \quad \mathbf{w}(r, \theta) = r^{1-\delta}\{-\delta(1 - \delta)\mathbf{F}(\theta)\mathbf{v}_0 + \mathbf{E}(\theta)\mathbf{w}_0\}, \tag{4a}$$

where

$$\mathbf{w}(r, \theta) = \begin{Bmatrix} \mathbf{u}(r, \theta) \\ \boldsymbol{\phi}(r, \theta) \end{Bmatrix}, \quad \mathbf{v}(r, \theta) = \begin{Bmatrix} T_{,r}(r, \theta) \\ h^*(r, \theta) \end{Bmatrix}, \quad \mathbf{w}_0 = \begin{Bmatrix} \mathbf{u}_0 \\ \boldsymbol{\phi}_0 \end{Bmatrix}, \quad \mathbf{v}_0 = \begin{Bmatrix} T_{0,r} \\ h_0^* \end{Bmatrix}. \quad (4b)$$

In (4), δ is the singular order and $\boldsymbol{\Gamma}(\theta)$, $\mathbf{F}(\theta)$, and $\mathbf{E}(\theta)$ are the matrices related to the material properties and corner angles and have different expressions for materials 1 and 2 (given in the Appendix). The eigenvectors associated with the singular order δ are \mathbf{w}_0 and \mathbf{v}_0 , and can be determined by

$$\mathbf{K}_e^{(3)} \mathbf{u}_0 = \mathbf{0}, \quad \boldsymbol{\phi}_0 = \mathbf{0}, \quad \mathbf{v}_0 = \mathbf{0}, \quad (5a)$$

where $\mathbf{K}_e^{(3)}$ is a 3×3 submatrix of \mathbf{K}_e defined by

$$\mathbf{K}_e = \begin{bmatrix} \mathbf{K}_e^{(1)} & \mathbf{K}_e^{(2)} \\ \mathbf{K}_e^{(3)} & \mathbf{K}_e^{(4)} \end{bmatrix}, \quad \mathbf{K}_e = \hat{\mathbf{N}}_2^{1-\delta}(\theta_2, \theta_1) \hat{\mathbf{N}}_1^{1-\delta}(\theta_1, \theta_0), \quad (5b)$$

and $\hat{\mathbf{N}}$ is the key matrix introduced in [Hwu et al. 2003]. In (4) and hereafter, the subscript k denoting the values related to the k -th material is dropped to lighten the notation.

In (5a), the equalities $\mathbf{K}_e^{(3)} \mathbf{u}_0 = \mathbf{0}$ and $\boldsymbol{\phi}_0 = \mathbf{0}$ come from the traction-free boundary condition set in (2b), and $\mathbf{v}_0 = \mathbf{0}$ comes from the requirement that the temperature is not allowed to be singular near the corner tip. From (4a) we see that if $\mathbf{v}_0 \neq \mathbf{0}$, both temperature and heat flux will be singular if the stresses are singular. If the stresses are singular and the strain energy cannot be unbounded, only the singular orders located in $0 < \text{Re}(\delta) < 1$ are considered in this paper.

With $\mathbf{v}_0 = \mathbf{0}$, the near-tip solutions (4a) become

$$\mathbf{v}(r, \theta) = \mathbf{0}, \quad \mathbf{w}(r, \theta) = r^{1-\delta} \mathbf{E}(\theta) \mathbf{w}_0, \quad (6)$$

which are the solutions without considering thermal effects. Since the singular order δ may be distinct or repeated, real or complex, combination of all the possible solutions associated with the most critical singular order whose real part δ_R is maximal leads, as in [Hwu and Kuo 2007; Hwu and Ikeda 2008], from (6) to

$$\begin{aligned} T(r, \theta) &= 0, & h_i(r, \theta) &= 0, \\ \mathbf{u}(r, \theta) &= \frac{1}{\sqrt{2\pi}} r^{1-\delta_R} \mathbf{V}(\theta) \langle (1 - \delta_R + i\epsilon_\alpha)^{-1} (r/l)^{i\epsilon_\alpha} \rangle \boldsymbol{\Lambda}^{-1} \mathbf{k}, \\ \boldsymbol{\phi}(r, \theta) &= \frac{1}{\sqrt{2\pi}} r^{1-\delta_R} \boldsymbol{\Lambda}(\theta) \langle (1 - \delta_R + i\epsilon_\alpha)^{-1} (r/l)^{i\epsilon_\alpha} \rangle \boldsymbol{\Lambda}^{-1} \mathbf{k}. \end{aligned} \quad (7)$$

In (7) the angular brackets $\langle \rangle$ stand for a diagonal matrix in which each component is varied according to the subscript α , for example, $\langle z_\alpha \rangle = \text{diag}[z_1, z_2, z_3]$; δ_R and ϵ_α are, respectively, the real and imaginary parts of the *most critical singular order* δ_c determined by (5a) with $0 < \text{Re}(\delta) < 1$; l is a length parameter which may be chosen arbitrarily as long as it is held fixed when specimens of a given material pair are compared; $\mathbf{V}(\theta)$ and $\boldsymbol{\Lambda}(\theta)$ are *eigenfunction matrices* related to $\mathbf{E}(\theta) \mathbf{w}_0$; $\boldsymbol{\Lambda} = \boldsymbol{\Lambda}(0)$, detailed expressions for which can be found in [Hwu and Kuo 2007; Kuo and Hwu 2010]; and \mathbf{k} is a vector containing different

modes of *stress intensity factors* and is defined by

$$\mathbf{k} = \begin{Bmatrix} K_{II} \\ K_I \\ K_{III} \end{Bmatrix} = \lim_{\substack{r \rightarrow 0 \\ \theta = 0}} \sqrt{2\pi} r^{\delta R} \mathbf{\Lambda} \langle (r/l)^{-i\epsilon_\alpha} \rangle \mathbf{\Lambda}^{-1} \begin{Bmatrix} \sigma_{r\theta} \\ \sigma_{\theta\theta} \\ \sigma_{3\theta} \end{Bmatrix}. \quad (8)$$

4. Path-independent H-integral for thermoelastic problems

According to the definition of stress intensity factors (8), to calculate their values we need to know the stresses near the tips of interface corners. However, due to the singular and possibly oscillatory behaviors of the near-tip stresses, it is not easy to get convergent values for the stress intensity factors directly from the definition (8). To overcome this problem, several path-independent integrals have been proposed for crack problems such as the J-integral [Rice 1968], the L-integral [Choi and Earmme 1992], the M-integral [Im and Kim 2000], and the H-integral [Bueckner 1973; Stern 1976; Sinclair et al. 1984; Chen 1985]. For corner problems that are usually in the status of mixed-mode intensity, the H-integral was suggested by [Hwu and Kuo 2007] for two-dimensional interface corners, and modified by [Kuo and Hwu 2010] for three-dimensional interface corners, which are valid for pure mechanical loading conditions. For interface corners under thermal loadings, the H-integral was modified by [Banks-Sills and Ishbir 2004; Nomura et al. 2009]. However, some important details that should be clarified were not interpreted in their works, such as the near-tip temperature field and the reason why the thermal effect disappears in near-tip solutions of displacements and stresses. Their H-integral cannot calculate the mixed-mode stress intensity factors via one expression. To have a complete picture of the H-integral for thermoelastic problems, in this section we first prove the path-independence property for the proposed modified H-integral, then provide a special treatment for the extra domain integral added in the modified H-integral.

4.1. Path-independence of the modified H-integral. If an elastic body is subjected to two different thermal loading systems (indicated by a hat or its absence), the constitutive laws shown in (1) give

$$\int_V \hat{\sigma}_{ij} \epsilon_{ij} dV = \int_V (C_{ijks} \hat{\epsilon}_{ks} \epsilon_{ij} - \beta_{ij} \hat{T} \epsilon_{ij}) dV, \quad (9a)$$

$$\int_V \sigma_{ij} \hat{\epsilon}_{ij} dV = \int_V (C_{ijks} \epsilon_{ks} \hat{\epsilon}_{ij} - \beta_{ij} T \hat{\epsilon}_{ij}) dV. \quad (9b)$$

Subtracting (9a) from (9b) and using the symmetry property of elastic constants, we get a conservative integral for thermoelastic problems,

$$\int_V (\hat{\sigma}_{ij} \epsilon_{ij} - \sigma_{ij} \hat{\epsilon}_{ij}) dV + \int_V \beta_{ij} (\hat{T} \epsilon_{ij} - T \hat{\epsilon}_{ij}) dV = 0. \quad (10a)$$

If one prefers the use of stresses instead of strains, (10a) can be rewritten as

$$\int_V (\hat{\sigma}_{ij} \epsilon_{ij} - \sigma_{ij} \hat{\epsilon}_{ij}) dV + \int_V \alpha_{ij} (\hat{T} \sigma_{ij} - T \hat{\sigma}_{ij}) dV = 0, \quad (10b)$$

where α_{ij} are the thermal expansion coefficients which are related to the thermal moduli β_{ij} by

$$\beta_{ij} = C_{ijks} \alpha_{ks}. \quad (11)$$

By using the strain-displacement relation (1)₃, the symmetric property of stresses, Cauchy's formula $t_i = \sigma_{ij}n_j$, and Gauss's divergence theorem $\int_V(\dots)_{,j}dV = \int_\Gamma(\dots)n_jd\Gamma$, the first domain integral in (10a) can be further reduced to a path integral, and consequently the following relation can be obtained

$$\int_\Gamma(\hat{t}_i u_i - t_i \hat{u}_i)d\Gamma + \int_V \beta_{ij}(\hat{T}\epsilon_{ij} - T\hat{\epsilon}_{ij})dV = 0. \quad (12)$$

In (12), Γ can be any positively oriented closed contour in a simply connected region. If Γ is selected to be $-\Gamma_\rho + \Gamma_1 + \Gamma_R + \Gamma_2$ and $V (= V_R - V_\rho)$ is the domain enclosed by Γ (see Figure 1), due to the traction-free condition on the corner flanks, that is, $t_i = \hat{t}_i = 0$ along Γ_1 and Γ_2 , (12) now leads to

$$\int_{\Gamma_\rho}(\hat{t}_i u_i - t_i \hat{u}_i)d\Gamma + \int_{V_\rho} \beta_{ij}(\hat{T}\epsilon_{ij} - T\hat{\epsilon}_{ij})dV = \int_{\Gamma_R}(\hat{t}_i u_i - t_i \hat{u}_i)d\Gamma + \int_{V_R} \beta_{ij}(\hat{T}\epsilon_{ij} - T\hat{\epsilon}_{ij})dV, \quad (13)$$

which means that the following modified H-integral is path-independent:

$$H = \int_{\Gamma_R}(\mathbf{u}^T \hat{\mathbf{t}} - \hat{\mathbf{u}}^T \mathbf{t})d\Gamma + \int_{V_R} \beta_{ij}(\hat{T}\epsilon_{ij} - T\hat{\epsilon}_{ij})dV. \quad (14)$$

The superscript T denotes a transpose; Γ_R is a counterclockwise integral path with arbitrary shape which emanates from the lower corner flank ($\theta = \theta_0$) and terminates on the upper flank ($\theta = \theta_2$); \mathbf{u} and \mathbf{t} are the displacement and traction vectors of the actual system, which can be obtained through any method, for example, finite element analyses, boundary element analyses, or even experimental measurement, while $\hat{\mathbf{u}}$ and $\hat{\mathbf{t}}$ are those of the auxiliary system with singular order $2 - \delta$.

In order to use the path-independence property of the modified H-integral to calculate the stress intensity factors, we can first select Γ_R to be a circular path which passes the region dominated by the singular field. Along the circular path, we have

$$\mathbf{t} = \boldsymbol{\phi}_{,\theta}/r \quad \text{and} \quad d\Gamma = r d\theta;$$

and hence (14) can be rewritten as

$$H = \int_{\theta_0}^{\theta_2}(\mathbf{u}^T \hat{\boldsymbol{\phi}}_{,\theta} - \hat{\mathbf{u}}^T \boldsymbol{\phi}_{,\theta})d\theta + \int_V \beta_{ij}(\hat{T}\epsilon_{ij} - T\hat{\epsilon}_{ij})dV, \quad (15)$$

in which \mathbf{u} , $\boldsymbol{\phi}$, ϵ_{ij} , and T are the near-tip solutions given in (7), and $\hat{\mathbf{u}}$, $\hat{\boldsymbol{\phi}}$, $\hat{\epsilon}_{ij}$, and \hat{T} are the auxiliary solutions, which can be obtained by

$$\hat{\mathbf{u}}(r, \theta) = r^{\delta_R-1} \hat{\mathbf{V}}(\theta) \langle r^{-i\epsilon_\alpha} \rangle \hat{\mathbf{c}}, \quad \hat{\boldsymbol{\phi}}(r, \theta) = r^{\delta_R-1} \hat{\boldsymbol{\Lambda}}(\theta) \langle r^{-i\epsilon_\alpha} \rangle \hat{\mathbf{c}}, \quad \hat{T}(r, \theta) = 0. \quad (16)$$

Since the temperature fields in both the near-tip and auxiliary solutions are zero, the H-integral passing through the singular field will be exactly the same as that for the pure mechanical loading problems. Since the relation between the stress intensity factors \mathbf{k} and the H-integral is obtained from the results of the H-integral passing through the singular field, it can now be written by referring to the relation obtained for the pure mechanical loading problem [Hwu and Kuo 2007], that is,

$$\mathbf{k} = \sqrt{2\pi} \boldsymbol{\Lambda} \langle (1 - \delta_R + i\epsilon_\alpha) l^{i\epsilon_\alpha} \rangle \mathbf{H}^{*-1} \mathbf{h}, \quad (17a)$$

where

$$\mathbf{H}^* = \int_{\theta_0}^{\theta_2} [\hat{\mathbf{A}}'^T(\theta) \mathbf{V}(\theta) - \hat{\mathbf{V}}^T(\theta) \mathbf{\Lambda}'(\theta)] d\theta, \quad \mathbf{h} = \begin{Bmatrix} H_1 \\ H_2 \\ H_3 \end{Bmatrix}. \quad (17b)$$

In (17b), the prime ' denotes differentiation with respect to θ ; H_i , $i = 1, 2, 3$, are the values of H calculated from (14) using the auxiliary solutions given in (16) with $\hat{c}_i = 1$ and $\hat{c}_j = 0$, $i \neq j$. Since the path-independence property has been proved through (13), the integral path calculating H_i can be chosen arbitrarily and \mathbf{u} , \mathbf{t} , and T of the actual system can be provided through any method, such as finite element analysis.

4.2. Special treatment of the extra domain integral. The difference between the modified H-integral (14) and the H-integral for the pure mechanical loading problem is the additional domain integral in the second term of (14). By selecting the auxiliary temperature field $\hat{T} = 0$, the domain integral becomes

$$- \int_{V_R} T \beta_{ij} \hat{\epsilon}_{ij} dV. \quad (18)$$

From the auxiliary solutions given in (16), we see that the auxiliary strain $\hat{\epsilon}_{ij}$ has a strong singularity as $r^{\delta-2}$, where $0 < \text{Re}(\delta) < 1$. This term will cause tremendous numerical error and hence should be treated with special attention. Banks-Sills and Ishbir [2004] proposed that the domain V_R can be separated into two parts: one is close to the corner tip, V_ρ in Figure 1, which can be integrated analytically, and the other adjacent part, $V = V_R - V_\rho$ in Figure 1, can be calculated numerically. However, in their study no analytical solution has been provided for the near-tip solution of temperature field, and hence no further analytical solution was provided for the integration. In [Nomura et al. 2009], this domain integral was calculated analytically for a circular integral path in which the circular sector domain is divided into several small elements whose temperature is assumed to be constant in each element. In the present study, the analytical integration is further simplified by using the near-tip solution of the temperature field.

Based upon the analytical solutions given in (4a) we see that the near-tip solution of the temperature field can be obtained by integrating (4a)₁ with respect to r , which will lead to

$$T(r, \theta) = (1 - \delta_h) r^{-\delta_h} \gamma(\theta) c_1 + c_2, \quad (19)$$

where $\gamma(\theta)$ is a function related to $\Gamma(\theta)$ of (4a); c_1 and c_2 are the coefficients to be determined via the actual temperature field which can come from analytical solution or numerical analysis. Here, δ_h is the *singular order of heat flux*, which is located in the region of $-1 < \text{Re}(\delta_h) < 0$ and will not induce a singularity in temperature or stresses.

According to the thermal conditions on the corner flanks (2c), the singular orders of heat flux have been obtained from the following relations [Hwu and Lee 2004]:

$$\begin{aligned} \text{isothermal-isothermal: } K_T^{(2)} &= 0, & \text{insulated-insulated: } K_T^{(3)} &= 0, \\ \text{insulated-isothermal: } K_T^{(1)} &= 0, & \text{isothermal-insulated: } K_T^{(4)} &= 0, \end{aligned} \quad (20)$$

where $K_T^{(i)}$, $i = 1, 2, 3, 4$, are the components of \mathbf{K}_T , which is a 2×2 matrix related to the heat conduction coefficients and corner angles.

To evaluate (18) analytically for the part of V_ρ , the auxiliary strain $\hat{\epsilon}_{ij}$ obtained from (16) can be expressed as

$$\begin{aligned}\hat{\epsilon}_{11} &= \mathbf{i}_1^T \hat{\mathbf{u}}_{,1}, & \hat{\epsilon}_{22} &= \mathbf{i}_2^T \hat{\mathbf{u}}_{,2}, & \hat{\epsilon}_{33} &= 0, \\ \hat{\epsilon}_{12} &= \frac{1}{2}(\mathbf{i}_2^T \hat{\mathbf{u}}_{,1} + \mathbf{i}_1^T \hat{\mathbf{u}}_{,2}), & \hat{\epsilon}_{23} &= \frac{1}{2}\mathbf{i}_3^T \hat{\mathbf{u}}_{,2}, & \hat{\epsilon}_{13} &= \frac{1}{2}\mathbf{i}_3^T \hat{\mathbf{u}}_{,1},\end{aligned}\quad (21a)$$

where

$$\begin{aligned}\hat{\mathbf{u}}_{,1} &= r^{\delta_R-2}(\cos\theta \mathbf{e}_1 - \sin\theta \mathbf{e}_2), & \hat{\mathbf{u}}_{,2} &= r^{\delta_R-2}(\sin\theta \mathbf{e}_1 + \cos\theta \mathbf{e}_2), \\ \mathbf{i}_1^T &= [1 \ 0 \ 0], & \mathbf{i}_2^T &= [0 \ 1 \ 0], & \mathbf{i}_3^T &= [0 \ 0 \ 1],\end{aligned}\quad (21b)$$

and

$$\mathbf{e}_1 = \hat{\mathbf{V}}(\theta) \langle (\delta_R - 1 - i\epsilon_\alpha) r^{-i\epsilon_\alpha} \rangle \hat{\mathbf{c}}, \quad \mathbf{e}_2 = \hat{\mathbf{V}}'(\theta) \langle r^{-i\epsilon_\alpha} \rangle \hat{\mathbf{c}}. \quad (21c)$$

Substituting (19) and (21) into (18), and letting $dV = r dr d\theta$ for V_ρ , we get

$$\int_{V_R} T \beta_{ij} \hat{\epsilon}_{ij} dV = I_\rho + \int_{V_R - V_\rho} T \beta_{ij} \hat{\epsilon}_{ij} dV, \quad (22a)$$

where I_ρ is the integral that has been integrated analytically with respect to r in the near-tip domain V_ρ whose result is

$$I_\rho = \rho^{\delta_R} \int_{\theta_0}^{\theta_2} e_0(\rho, \theta) d\theta, \quad (22b)$$

in which

$$e_0(\rho, \theta) = \boldsymbol{\beta}_1^{*T}(\theta) \hat{\mathbf{V}}(\theta) \langle (\delta_R - 1 - i\epsilon_\alpha) g_\alpha(\rho, \theta) \rangle \hat{\mathbf{c}} + \boldsymbol{\beta}_2^{*T}(\theta) \hat{\mathbf{V}}'(\theta) \langle g_\alpha(\rho, \theta) \rangle \hat{\mathbf{c}}, \quad (22c)$$

and

$$g_\alpha(\rho, \theta) = \left\{ \frac{c_1(1 - \delta_h)\rho^{-\delta_h}}{\delta_R - \delta_h - i\epsilon_\alpha} \gamma(\theta) + \frac{c_2}{\delta_R - i\epsilon_\alpha} \right\} \rho^{-i\epsilon_\alpha}, \quad (22d)$$

$$\boldsymbol{\beta}_1^*(\theta) = \cos\theta \boldsymbol{\beta}_1 + \sin\theta \boldsymbol{\beta}_2, \quad \boldsymbol{\beta}_2^*(\theta) = -\sin\theta \boldsymbol{\beta}_1 + \cos\theta \boldsymbol{\beta}_2, \quad \boldsymbol{\beta}_1 = \begin{Bmatrix} \beta_{11} \\ \beta_{12} \\ \beta_{13} \end{Bmatrix}, \quad \boldsymbol{\beta}_2 = \begin{Bmatrix} \beta_{21} \\ \beta_{22} \\ \beta_{23} \end{Bmatrix}. \quad (22e)$$

In (22a)–(22c), ρ is the radius of a small circle ahead of the corner tip. Since $0 < \delta_R < 1$ and $-1 < \text{Re}(\delta_h) < 0$, from the results of (22a)–(22e) we see that the singular problem of (18) has been solved through the analytical integration I_ρ . To have a proper choice of ρ , the convergent test about ρ should be done in a numerical calculation, which will be illustrated by an example shown in the next section. Since the singular problem in the near-tip domain occurs from approaching zero distance, that is, $r \rightarrow 0$, whether to obtain the analytical integration with respect to θ is not the main concern of our study. Therefore, due to the complexity of $\gamma(\theta)$ and $\hat{\mathbf{V}}(\theta)$ in $e_0(\rho, \theta)$, the analytical integration of I_ρ shown in (22b) is only for the variable r not including θ .

5. Numerical examples

To provide a stable and efficient computing approach for the general mixed-mode stress intensity factors under thermal loadings, the path-independent H-integral proposed in the literature [Hwu and Kuo 2007] has been modified by adding an extra domain integral as shown in (14). This integral is applicable to

cracks, interface cracks, corners, and interface corners, and the materials containing the cracks/corners can be any kinds of anisotropic materials, including degenerate materials such as isotropic materials. The stress intensity factors calculated through the H-integral include the pure mode and mixed mode, and also the factors associated with lower singular orders [Kuo and Hwu 2010]. The main feature of the present approach is that one unified H-integral can deal with several different kinds of thermal problems which are generally discussed separately. Thus, to provide an enhanced comparison, several different kinds of materials and cracks/corners considered in the literature are shown in the following examples. In order to show that the modified H-integral is path-independent, the data shown below will be presented by stress intensity factors with different radius of integral path.

All the examples presented in this section consider the state of plane strain. The physical quantities of the actual system, \mathbf{u} , \mathbf{t} , and T , needed for the calculation of the H-integral in (14) are obtained from the commercial finite element software ANSYS. A two-dimensional 4-node thermal element PLANE55 is adopted to perform the thermal analyses, and then the temperature results are read into a two-dimensional 4-node structural solid element PLANE42 and treated as the body force to proceed with the stress analyses. Since the numerical output will depend on element meshes, the convergent test needs to be done before performing all the following examples. In our numerical implementation, the number of elements for the most refined mesh is 29574 for modeling the electronic package, and 7484 for modeling the interface crack. For convenience, the H-integral path doesn't need to pass through nodal points, while the integration points can be arbitrary points whose numerical data are produced by extrapolating the results of their surrounding nodal points [Lancaster and Salkauskas 1981; Nomura et al. 2009] and then integrated by Gaussian quadrature. Note that although the path-independence property of the H-integral has been proved theoretically in Section 4, when using the H-integral to calculate the stress intensity factors we still have to avoid taking the numerical results overly close to the corner tip due to the incorrect stress information in the neighborhood of the corner tip provided by finite element analysis. Also note that although the solution techniques proposed in this paper are applicable to the most general two-dimensional problems, such as the generalized plane strain and generalized plane stress, due to the limitation of two-dimensional elements provided by the finite element software ANSYS only the plane strain condition is considered in our examples.

5.1. Comparison with existing solutions. In order to prove the path-independence property numerically, to verify the correctness of the stress intensity factors calculated by the proposed H-integral and to show the versatility of the present unified approach, six different kinds of cracks/corners under thermal loadings are implemented and compared with the existing solutions presented in the literature. They are:

- Case 1: A center crack under mode I thermal loading (Figure 2, left).
- Case 2: A center crack under mixed-mode thermal loading (Figure 2, right).
- Case 3: A center interface crack under uniform heat flow (Figure 3, left).
- Case 4: Edge interface cracks under uniform temperature change (Figure 3, right).
- Case 5: Edge interface corners under uniform temperature change (Figure 4, left).
- Case 6: An interface corner under uniform temperature change (Figure 4, right).

Point A in Figures 2–4 stands for the corner or crack tip we are concerned with in these problems. The geometry, loading, and material properties of these problems are collected in Table 1. The results of

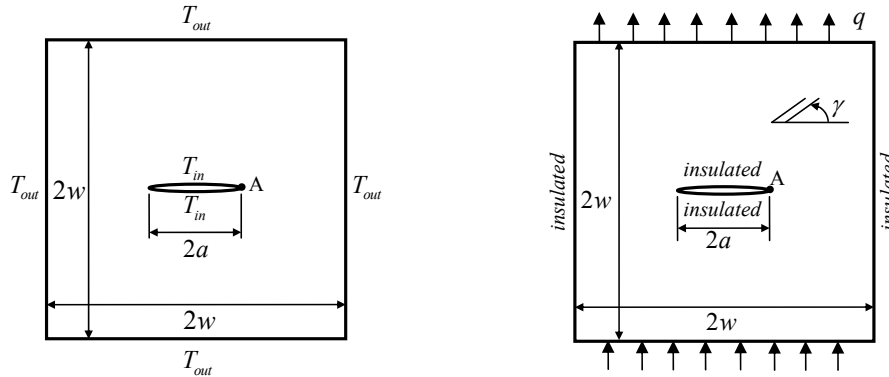


Figure 2. A center crack in a square plate under mode *I* (left, Case 1) and mixed-mode (right, Case 2) thermal loadings.

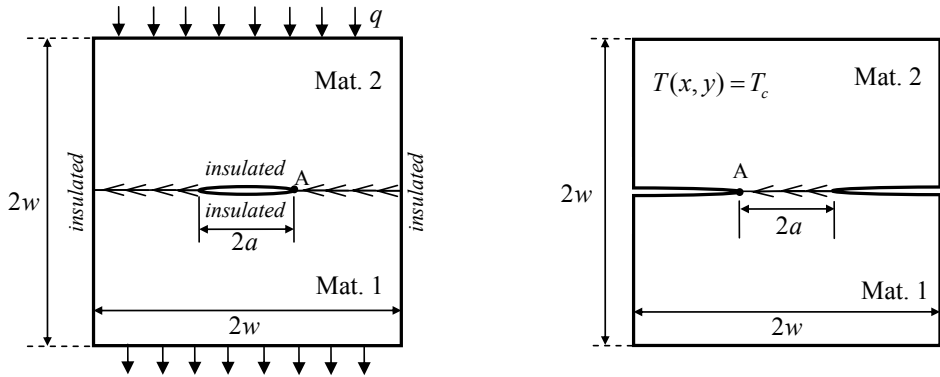


Figure 3. A center interface crack (left, Case 3) and edge interface cracks (right, Case 4) in a square bimaterial plate.

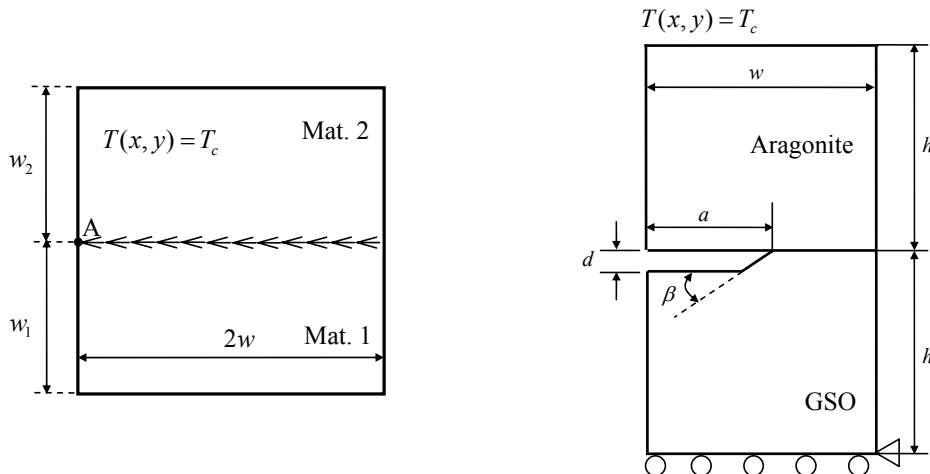


Figure 4. Edge interface corners (left, Case 5) and an interface corner (right, Case 6) in a bimaterial plate.

Case 1 (Figure 2, left) Center crack under mode I thermal loading, isotropic material			
$a = 4 \text{ mm}$	$w = 10a$	$T_{\text{in}} = 0^\circ\text{C}$	$T_{\text{out}} = 100^\circ\text{C}$
$E = 1 \text{ MPa}$	$\nu = 0.3$	$\alpha = 10^{-4} \text{ }^\circ\text{C}^{-1}$	$k = 1 \text{ W/m}^\circ\text{C}$
Case 2 (Figure 2, right) Center crack under mixed-modes thermal loading, orthotropic material ($\gamma = 0^\circ$), anisotropic material ($\gamma = 30^\circ$)			
$a = 1 \text{ mm}$	$w = 30a$	$q = 10^3 \text{ W/m}^2$	
$E_{11} = 144.23 \text{ GPa}$	$E_{22} = E_{33} = 9.65 \text{ GPa}$	$G_{12} = 4.14 \text{ GPa}$	$\alpha_{11} = 0.88 \times 10^{-6} \text{ }^\circ\text{C}^{-1}$
$\nu_{12} = \nu_{13} = 0.301$	$\nu_{23} = 0.49$	$G_{13} = 4.14 \text{ GPa}$	$\alpha_{22} = 31 \times 10^{-6} \text{ }^\circ\text{C}^{-1}$
$k_{11} = 4.48 \text{ W/m}^\circ\text{C}$	$k_{22} = k_{33} = 3.21 \text{ W/m}^\circ\text{C}$	$G_{23} = 3.45 \text{ GPa}$	$\alpha_{33} = 31 \times 10^{-6} \text{ }^\circ\text{C}^{-1}$
Case 3 (Figure 3, left) Center interface crack under uniform heat flow, isotropic bimetaterials			
$a = 4 \text{ mm}$	$w = 20a$	$q = 10^5 \text{ W/m}^2$	
$E_1 = 1000 \text{ GPa}$	$\nu_1 = 0.3$	$\alpha_1 = 10^{-6} \text{ }^\circ\text{C}^{-1}$	$k_1 = 100 \text{ W/m}^\circ\text{C}$
$E_2 = 100 \text{ GPa}$	$\nu_2 = 0.3$	$\alpha_2 = 10^{-7} \text{ }^\circ\text{C}^{-1}$	$k_2 = 100 \text{ W/m}^\circ\text{C}$
Case 4 (Figure 3, right) Edge interface crack under uniform temperature change, isotropic bimetaterials			
$a = 1 \text{ mm}$	$w = 100a$	$T_c = 100^\circ\text{C}$	
$E_1 = 1000 \text{ GPa}$	$\nu_1 = 0.3$	$\alpha_1 = 10^{-6} \text{ }^\circ\text{C}^{-1}$	
$E_2 = 100 \text{ GPa}$	$\nu_2 = 0.3$	$\alpha_2 = 10^{-7} \text{ }^\circ\text{C}^{-1}$	
Case 5 (Figure 4, left) Edge interface corner under uniform temperature change, isotropic bimetaterials			
$w = 1000 \text{ mm}$	$w_1 = 461 \text{ mm}$	$w_2 = 359 \text{ mm}$	$T_c = -100^\circ\text{C}$
$E_1 = 72 \text{ GPa}$	$\nu_1 = 0.3$	$\alpha_1 = 18.95 \times 10^{-6} \text{ }^\circ\text{C}^{-1}$	
$E_2 = 280 \text{ GPa}$	$\nu_2 = 0.26$	$\alpha_2 = 2.5 \times 10^{-6} \text{ }^\circ\text{C}^{-1}$	
Case 6 (Figure 4, right) Interface corner under uniform temperature change, anisotropic bimetaterials			
$a = 1.6 \text{ mm}, d = 0.1 \text{ mm}, h = 7.5 \text{ mm}, w = 3 \text{ mm}, \beta = 20^\circ, T_c = -20^\circ\text{C},$			
$\mathbf{C}_{\text{GSO}} = \begin{bmatrix} 223 & 108 & 98.5 & 0 & 84 & 0 \\ 150 & 102 & 0 & 33.3 & 0 & 0 \\ & 251 & 0 & -6 & 0 & 0 \\ \text{sym.} & & 78.8 & 0 & 6.6 & 0 \\ & & & 68.8 & 0 & 0 \\ & & & & 82.7 & 0 \end{bmatrix} [\text{GPa}],$		$\mathbf{C}_{\text{aragonite}} = \begin{bmatrix} 87.8 & 26.3 & 36.6 & 0 & 18.75 & 0 \\ & 87 & 26.3 & 0 & 10.35 & 0 \\ & & 87.8 & 0 & 18.75 & 0 \\ & & & 42 & 0 & 0.7 \\ \text{sym.} & & & & 60.27 & 0 \\ & & & & & 42 \end{bmatrix} [\text{GPa}],$	
$\alpha_{\text{GSO}} = \begin{bmatrix} 4.4 & 0 & 0 \\ 0 & 14 & 0 \\ 0 & 0 & 6.8 \end{bmatrix} [10^{-6} \text{ }^\circ\text{C}^{-1}],$		$\alpha_{\text{aragonite}} = \begin{bmatrix} 22.5 & 0 & 0 \\ 0 & 17 & 0 \\ 0 & 0 & 22.5 \end{bmatrix} [10^{-6} \text{ }^\circ\text{C}^{-1}],$	

Table 1. Geometries, loading, and material properties of numerical examples.

the order of stress singularity δ , the order of heat flux singularity δ_h , the stress intensity factors K_I and K_{II} versus the radius of path integral r/a , and the reference solutions are all shown in Table 2.

From this table we see that the results calculated by the present approach are not only path-independent but also agree well with those presented in the literature for all different cases, for example, Case 1 [Sumi and Katayama 1980; Maiti 1992; Mukhopadhyay et al. 1999], Case 2 [Hwu 1990], Case 3 [Banks-Sills and Dolev 2004], Case 4 [Erdogan 1965], and Case 5 [Banks-Sills and Ishbir 2004]. In Case 6, due to the limitations of two-dimensional elements of ANSYS only the plane strain condition is considered, and hence in our example the thermal expansion coefficient α_{13} considered in the reference paper [Nomura et al. 2009], which may induce deformation in the third direction, is neglected. With this neglect, as shown in Table 2 our results are slightly different from those presented in [Nomura et al. 2009]. Table 3

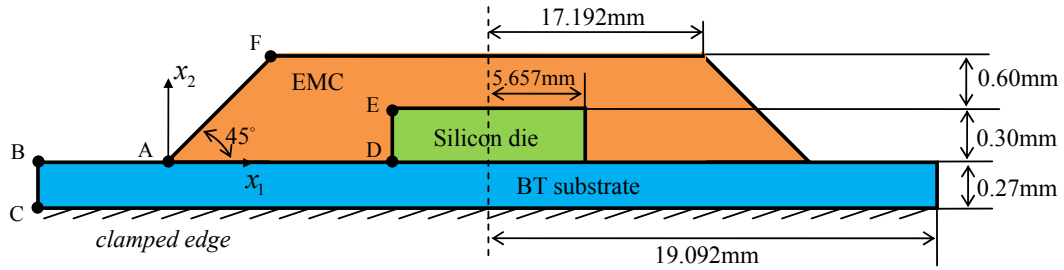


Figure 5. A sample electronic package.

Case	Singular order		r/a	K_I (MPa \times mm $^{\delta_R}$)		K_{II} (MPa \times mm $^{\delta_R}$)	
	δ	δ_h		Present	Reference	Present	Reference
1	0.5	-0.5	0.3	0.01722	0.01739 ^[1]	0	
			0.6	0.01722	0.01695 ^[2]	0	0
			0.8	0.01722	0.01722 ^[3]	0	
2	0.5	-0.5	(Orthotropic material)				
			0.3	0		-0.02699	
			0.6	0	0	-0.02702	-0.02693 ^[4]
			0.8	0		-0.02700	
			(Anisotropic material)				
			0.3	0.01147		-0.03375	
0.6	0.01148	0.01150 ^[4]	-0.03375	-0.03357 ^[4]			
0.8	0.01148		-0.03376				
3*	0.5 + 0.076i	-0.5	0.3	-1.611×10^5		-8.890×10^3	
			0.6	-1.615×10^5	-1.636×10^5 ^[5]	-8.850×10^3	-8.908×10^3 ^[5]
			0.8	-1.615×10^5		-8.817×10^3	
4*	0.5 + 0.076i	-0.5	0.3	-1.559		10.65	
			0.6	-1.577	-1.526 ^[6]	10.69	10.07 ^[6]
			0.9	-1.537		10.63	
5**	0.111	-1	0.03	1.867×10^3		-317.6	
			0.06	1.869×10^3	1.848×10^3 ^[7]	-317.9	-
			0.09	1.867×10^3		-317.5	
6***	0.482 + 0.041i	-	0.6	3.540		16.67	
			0.8	3.572	3.278 ^[8]	16.47	22.90 ^[8]

δ : order of stress singularity; δ_h : order of heat flux singularity; δ_R : real part of stress singular order;

*: reference length l is selected to be $2a$; **: normalized factor a is replaced by $w = 1000$ mm in Figure 4, left;

***: reference length l is selected to be $10 \mu\text{m}$ and normalized factor a is replaced by $d = 0.1$ mm in Figure 4, right; ^[1] [Sumi and Katayama 1980]; ^[2] [Maiti 1992]; ^[3] [Mukhopadhyay et al. 1999]; ^[4] [Hwu 1990];

^[5] [Banks-Sills and Dolev 2004]; ^[6] [Erdogan 1965]; ^[7] [Banks-Sills and Ishbir 2004]; ^[8] [Nomura et al. 2009].

Table 2. Comparison of stress intensity factors.

ρ/a	$(r/a = 0.3)$		$(r/a = 0.6)$	
	$K_I(\text{GPa} \times \text{mm}^{0.5})$	$K_{II}(\text{GPa} \times \text{mm}^{0.5})$	$K_I(\text{GPa} \times \text{mm}^{0.5})$	$K_{II}(\text{GPa} \times \text{mm}^{0.5})$
0.0001	-161.2	-9.093	-161.4	-8.942
0.001	-161.3	-9.075	-161.5	-8.925
0.005	-161.1	-8.910	-161.5	-8.880
0.01	-161.1	-8.890	-161.5	-8.850
0.05	-161.2	-8.878	-161.5	-8.813
0.1	-161.4	-8.952	-161.6	-8.801
0.2	-161.6	-8.861	-161.8	-8.710
0.3	-161.9	-8.672		
0.4			-162.3	-8.236
0.5			-162.5	-7.856
0.6			-162.7	-7.381

Table 3. Effects of radius ρ on the stress intensity factors for Case 3.

shows the effects of the radius ρ of the small circle chosen for the analytical area integral of (22b). From this table, we see that the effect of ρ is very trifling on the results of the stress intensity factors when $\rho/a \leq 0.2$, and this phenomenon is consistent with the results presented in [Banks-Sills and Ishbir 2004]. Note that the bigger ρ is, the more mesh and computation time we can save, and this vindicates to the use of analytical integration in (22b).

5.2. Application to electronic packages. A typical example of electronic packages is shown in Figure 5. This package consists of three different parts: silicon die, epoxy molding compound (EMC), and bismaleimide triazine (BT) substrate. Their mechanical properties are shown in Table 4. Due to the discontinuity of geometries and/or material properties, stress concentration usually occurs at the corners or interface corners, such as points A, B, C, D, E, and F shown in Figure 5. To know which corner is the most critical corner, we first calculate the orders of stress/heat flux singularity. Table 5 shows the results of singular orders of these corners, in which the values of points A, B, and F are calculated from (5a)

Material	E [GPa]	ν	$\alpha [10^{-6} \text{ }^\circ\text{C}^{-1}]$	$k [\text{W/m }^\circ\text{C}]$
Silicon die	131	0.3	2.8	300
EMC	16	0.25	8	14
BT substrate	26	0.11	15	0.95

Table 4. Material properties of the sample electronic package.

Singular order	Location					
	A	B	C	D	E	F
δ	0.280	0	0.143	0.277	0.253	0
δ_h	-0.979	-1	-1	-0.894	-0.699	-1

Table 5. Orders of stress/heat flux singularity of the sample electronic package.

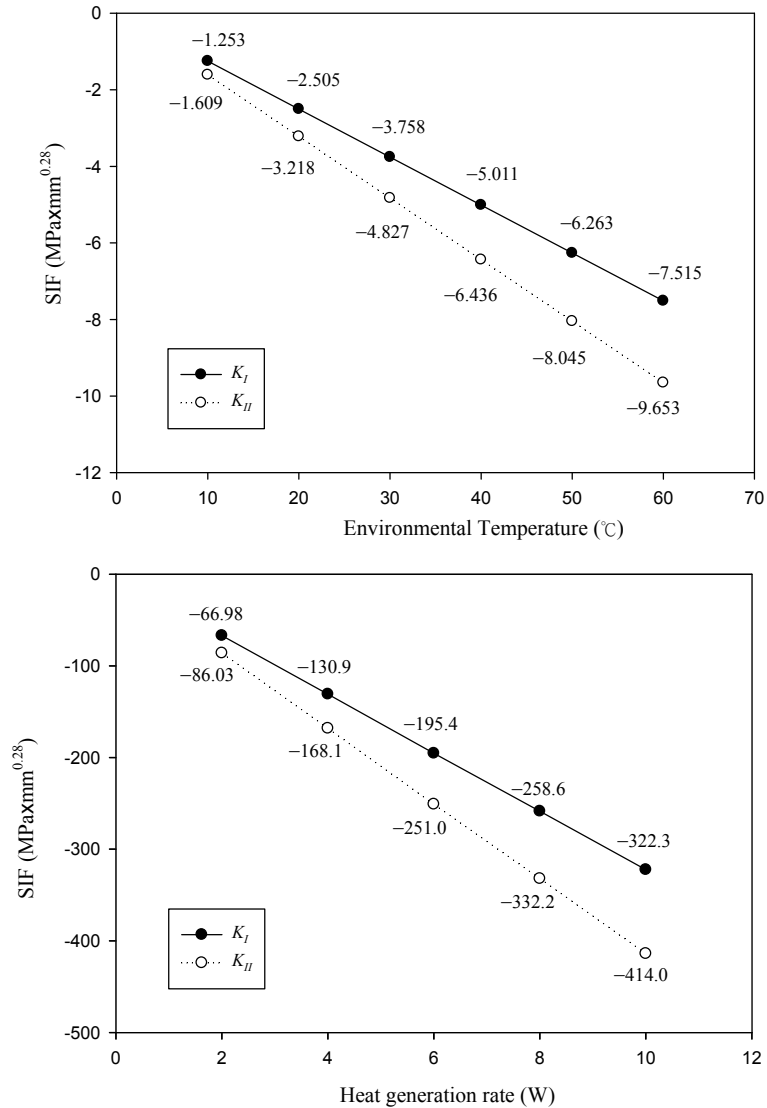


Figure 6. Stress intensity factors versus environmental temperature (top) and versus heat generation rate (bottom).

and (20), for stress and heat flux singularity respectively. For points C, D, and E, whose corner edges are not traction-free, related formulae can be found in [Hwu and Lee 2004]. From Table 5, we see that point A is the most critical point.

To study the effects of thermal environment on the stress intensity factors, we now consider two different thermal conditions: (1) the package is placed within an environmental temperature maintained at a constant temperature T_c , and the chip (silicon die) has a heat generation rate of 10 W; (2) the package is placed amid an environment with reference temperature $T_{\text{ref}} = 25^{\circ}\text{C}$ before the chip begins to generate heat, convection with heat transfer coefficient $10 \text{ W/m}^2\text{C}$ is imposed on all the outer edges, and the chip (silicon die) has a heat generation rate Q . It is assumed that this package doesn't deform at 0°C . By using

the modified H-integral proposed in this paper, the stress intensity factors associated with the singular order $\delta = 0.28$ of point A are calculated by varying T_c for the first case and varying Q for the second case. Figure 6 shows that both of the mode I and mode II stress intensity factors vary linearly with environmental temperature T_c and heat generation rate Q .

6. Conclusions

In this investigation, the modified H-integral is proposed to calculate the stress intensity factors of interface corners subjected to thermal loadings, and its required near-tip solutions and auxiliary solutions of displacements, stresses, and temperature are all provided. Through several different material types, corner types, and thermal loading types used in the numerical examples, the H-integral proves its validity and versatility in thermal problems. Moreover, the path-independence property of the modified H-integral in thermal problems has been proved both theoretically and numerically. A special treatment for the strongly singular function in the domain integral of the modified H-integral saves us a lot of computational time and also raises the accuracy for the calculation of stress intensity factors.

Appendix: Explicit expressions of the near-tip solutions

Under thermal effects, the field solutions near the tip of multimaterial wedges has been shown in Equation (53) of [Hwu and Lee 2004]. To explicitly show the r -dependent relation of the near-tip solutions by using Equation (27) of the same reference, we may let the solutions along the wedge surface $\theta = \theta_0$ be

$$v_1(\theta_0) = -\delta(1 - \delta)r^{-1-\delta}v_0, \quad w_1(\theta_0) = r^{1-\delta}w_0. \tag{A-1}$$

Substituting (A-1) into [Hwu and Lee 2004, (53)], the near-tip solutions can be expressed as those shown in (4a) and (4b), in which

$$\begin{aligned} \Gamma(\theta) &= \begin{cases} \Gamma_1^*(\theta) & \text{when } \theta_0 \leq \theta \leq \theta_1, \\ \Gamma_2^*(\theta)(\mathbf{K}_T)_1 & \text{when } \theta_1 \leq \theta \leq \theta_2, \end{cases} \\ \mathbf{E}(\theta) &= \begin{cases} \mathbf{E}_1^*(\theta) & \text{when } \theta_0 \leq \theta \leq \theta_1, \\ \mathbf{E}_2^*(\theta)(\mathbf{K}_e)_1 & \text{when } \theta_1 \leq \theta \leq \theta_2, \end{cases} \\ \mathbf{F}(\theta) &= \begin{cases} \mathbf{F}_1^*(\theta) & \text{when } \theta_0 \leq \theta \leq \theta_1, \\ \mathbf{F}_2^*(\theta)(\mathbf{K}_T)_1 + \mathbf{E}_2^*(\theta)(\mathbf{K}_c)_1 & \text{when } \theta_1 \leq \theta \leq \theta_2, \end{cases} \end{aligned} \tag{A-2}$$

where

$$\begin{aligned} \Gamma_k^*(\theta) &= \Theta_k \langle \hat{\tau}_\beta^{-\delta}(\theta, \theta_{k-1}) \rangle_k \Theta_k^{-1}, \quad \mathbf{E}_k^*(\theta) = \hat{\mathbf{N}}_k^{1-\delta}(\theta, \theta_{k-1}), \\ \mathbf{F}_k^*(\theta) &= \frac{1}{\delta(1-\delta)} \{ \hat{\mathbf{N}}_k^{1-\delta}(\theta, \theta_{k-1}) \mathbf{U}_k - \mathbf{U}_k \langle \hat{\tau}_\beta^{1-\delta}(\theta, \theta_{k-1}) \rangle_k \langle \hat{\tau}_\beta^{1-\delta}(\theta_{k-1}, 0) \rangle_k \Theta_k^{-1}, \quad k = 1, 2, \end{aligned} \tag{A-3}$$

and

$$\begin{aligned}
 (\mathbf{K}_T)_1 &= \mathbf{\Gamma}_1^*(\theta_1), \quad (\mathbf{K}_e)_1 = \mathbf{E}_1^*(\theta_1), \quad (\mathbf{K}_c)_1 = \mathbf{F}_1^*(\theta_1), \\
 \mathbf{\Theta}_k &= \begin{bmatrix} 1 & 1 \\ -ik_0 & ik_0 \end{bmatrix}_k, \quad \mathbf{U}_k = \begin{bmatrix} \mathbf{c}_k & \bar{\mathbf{c}}_k \\ \mathbf{d}_k & \bar{\mathbf{d}}_k \end{bmatrix}, \\
 \hat{\mathbf{N}}_k^{1-\delta}(\theta, \theta') &= \begin{bmatrix} \mathbf{A}_k & \bar{\mathbf{A}}_k \\ \mathbf{B}_k & \bar{\mathbf{B}}_k \end{bmatrix} \begin{bmatrix} \langle \hat{\mu}_\alpha^{1-\delta}(\theta, \theta') \rangle_k & \mathbf{0} \\ \mathbf{0} & \langle \hat{\mu}_\alpha^{1-\delta}(\theta, \theta') \rangle_k \end{bmatrix} \begin{bmatrix} \mathbf{B}_k^T & \mathbf{A}_k^T \\ \bar{\mathbf{B}}_k^T & \bar{\mathbf{A}}_k^T \end{bmatrix}, \quad (\text{A-4})
 \end{aligned}$$

$$\hat{\mu}_\alpha(\theta, \theta') = \cos(\theta - \theta') + \sin(\theta - \theta')\mu_\alpha(\theta'), \quad \mu_\alpha(\theta') = \frac{\mu_\alpha \cos \theta' - \sin \theta'}{\mu_\alpha \sin \theta' + \cos \theta'}, \quad \alpha = 1, 2, 3,$$

$$\hat{\tau}_\beta(\theta, \theta') = \cos(\theta - \theta') + \sin(\theta - \theta')\tau_\beta(\theta'), \quad \tau_\beta(\theta') = \frac{\tau_\beta \cos \theta' - \sin \theta'}{\tau_\beta \sin \theta' + \cos \theta'}, \quad \beta = 1, 2,$$

In (A-2)–(A-4), subscript k (taking the values 1, 2) denotes the quantities related to the k -th wedge, whereas subscript α and β denote the diagonal components of the diagonal matrix. $i = \sqrt{-1}$ is an imaginary unit; a bar above a letter denotes complex conjugation; k_0 is a real constant related to the heat conduction coefficients k_{ij} by

$$k_0 = \sqrt{k_{11}k_{22} - k_{12}^2}; \quad (\text{A-5})$$

μ_α and τ_β are the elastic eigenvalues and thermal eigenvalues; and \mathbf{A} , \mathbf{B} and \mathbf{c} , \mathbf{d} are the elastic eigenvector matrices and thermal eigenvectors of the Stroh formalism of anisotropic elasticity; see [Ting 1996; Hwu 2010].

References

- [Banks-Sills and Dolev 2004] L. Banks-Sills and O. Dolev, “The conservative M -integral for thermal-elastic problems”, *Int. J. Fract.* **125**:1–2 (2004), 149–170.
- [Banks-Sills and Ishbir 2004] L. Banks-Sills and C. Ishbir, “A conservative integral for bimaterial notches subjected to thermal stresses”, *Int. J. Numer. Methods Eng.* **60**:6 (2004), 1075–1102.
- [Brown and Erdogan 1968] E. J. Brown and F. Erdogan, “Thermal stresses in bonded materials containing cuts on the interface”, *Int. J. Eng. Sci.* **6**:9 (1968), 517–529.
- [Bueckner 1973] H. F. Bueckner, “Field singularities and related integral representations”, pp. 239–314 in *Methods of analysis and solutions of crack problems: recent developments in fracture mechanics: theory and methods of solving crack problems*, edited by G. C. Sih, Mechanics of Fracture **1**, Noordhoff, Leyden, 1973.
- [Chen 1985] Y. Z. Chen, “New path independent integrals in linear elastic fracture mechanics”, *Eng. Fract. Mech.* **22**:4 (1985), 673–686.
- [Choi and Earmme 1992] N. Y. Choi and Y. Y. Earmme, “Evaluation of stress intensity factors in circular arc-shaped interfacial crack using L integral”, *Mech. Mater.* **14**:2 (1992), 141–153.
- [Clements 1973] D. L. Clements, “Thermal stress in an anisotropic elastic half-space”, *SIAM J. Appl. Math.* **24**:3 (1973), 332–337.
- [Erdogan 1965] F. Erdogan, “Stress distribution in bonded dissimilar materials with cracks”, *J. Appl. Mech. (ASME)* **32** (1965), 403–410.
- [Hwu 1990] C. Hwu, “Thermal stresses in an anisotropic plate disturbed by an insulated elliptic hole or crack”, *J. Appl. Mech. (ASME)* **57**:4 (1990), 916–922.

- [Hwu 1992] C. B. Hwu, "Thermoelastic interface crack problems in dissimilar anisotropic media", *Int. J. Solids Struct.* **29**:16 (1992), 2077–2090.
- [Hwu 2010] C. Hwu, *Anisotropic elastic plates*, Springer, New York, 2010.
- [Hwu and Ikeda 2008] C. Hwu and T. Ikeda, "Electromechanical fracture analysis for corners and cracks in piezoelectric materials", *Int. J. Solids Struct.* **45**:22–23 (2008), 5744–5764.
- [Hwu and Kuo 2007] C. Hwu and T. L. Kuo, "A unified definition for stress intensity factors of interface corners and cracks", *Int. J. Solids Struct.* **44**:18–19 (2007), 6340–6459.
- [Hwu and Lee 2004] C. Hwu and W.-J. Lee, "Thermal effect on the singular behavior of multibonded anisotropic wedges", *J. Therm. Stresses* **27**:2 (2004), 111–136.
- [Hwu et al. 2003] C. Hwu, M. Omiya, and K. Kishimoto, "A key matrix N for the stress singularity of the anisotropic elastic composite wedges", *JSME Int. J. A Mech. M.* **46**:1 (2003), 40–50.
- [Ikeda and Sun 2001] T. Ikeda and C. T. Sun, "Stress intensity factor analysis for an interface crack between dissimilar isotropic materials under thermal stress", *Int. J. Fract.* **111**:3 (2001), 229–249.
- [Im and Kim 2000] S. Im and K.-S. Kim, "An application of two-state M -integral for computing the intensity of the singular near-tip field for a generic wedge", *J. Mech. Phys. Solids* **48**:1 (2000), 129–151.
- [Kuo and Hwu 2010] T.-L. Kuo and C. Hwu, "Multi-order stress intensity factors along three-dimensional interface corners", *J. Appl. Mech. (ASME)* **77**:3 (2010), 031020.
- [Lancaster and Salkauskas 1981] P. Lancaster and K. Salkauskas, "Surfaces generated by moving least squares methods", *Math. Comput.* **37** (1981), 141–158.
- [Maiti 1992] S. K. Maiti, "A finite element for variable order singularities based on the displacement formulation", *Int. J. Numer. Methods Eng.* **33**:9 (1992), 1955–1974.
- [Mukhopadhyay et al. 1999] N. K. Mukhopadhyay, S. K. Maiti, and A. Kakodkar, "Modified crack closure integral based computation of stress intensity factors for 2-D thermoelastic problems through boundary element method", *Nucl. Eng. Des.* **187**:3 (1999), 277–290.
- [Munz and Yang 1992] D. Munz and Y. Y. Yang, "Stress singularities at the interface in bonded dissimilar materials under mechanical and thermal loading", *J. Appl. Mech. (ASME)* **59**:4 (1992), 857–861.
- [Munz and Yang 1993] D. Munz and Y. Y. Yang, "Stresses near the edge of bonded dissimilar materials described by two stress intensity factors", *Int. J. Fract.* **60**:2 (1993), 169–177.
- [Nagai et al. 2007] M. Nagai, T. Ikeda, and N. Miyazaki, "Stress intensity factor analysis of an interface crack between dissimilar anisotropic materials under thermal stress using the finite element analysis", *Int. J. Fract.* **146**:4 (2007), 233–248.
- [Nomura et al. 2009] Y. Nomura, T. Ikeda, and N. Miyazaki, "Stress intensity factor analysis at an interfacial corner between anisotropic bimetals under thermal stress", *Eng. Fract. Mech.* **76**:2 (2009), 221–235.
- [Nowacki 1962] W. Nowacki, *Thermoelasticity*, Addison-Wesley, Reading, MA, 1962.
- [Rice 1968] J. R. Rice, "A path independent integral and the approximate analysis of strain concentration by notches and cracks", *J. Appl. Mech. (ASME)* **35** (1968), 379–386.
- [Sinclair et al. 1984] G. B. Sinclair, M. Okajima, and J. H. Griffen, "Path independent integrals for computing stress intensity factors at sharp notches in elastic plates", *Int. J. Numer. Methods Eng.* **20**:6 (1984), 999–1008.
- [Stern 1976] M. Stern, "A boundary integral representation for stress intensity factors", pp. 125–132 in *Recent advances in engineering science* (Raleigh, NC, 1973), vol. 7, edited by T. S. Chang, Scientific Publishers, Boston, 1976.
- [Stroh 1958] A. N. Stroh, "Dislocations and cracks in anisotropic elasticity", *Philos. Mag.* **3**:30 (1958), 625–646.
- [Sumi and Katayama 1980] N. Sumi and T. Katayama, "Thermal stress singularities at tips of a Griffith crack in a finite rectangular plate", *Nucl. Eng. Des.* **60**:3 (1980), 389–394.
- [Ting 1996] T. C. T. Ting, *Anisotropic elasticity: theory and applications*, Oxford Engineering Science Series **45**, Oxford University Press, New York, 1996.

CHYANBIN HWU: chwu@mail.ncku.edu.tw

Institute of Aeronautics and Astronautics, National Cheng Kung University, No.1, University Road, Tainan 70101, Taiwan

TAI-LIANG KUO: kelvenkiss@yahoo.com.tw

Institute of Aeronautics and Astronautics, National Cheng Kung University, No.1, University Road, Tainan 70101, Taiwan

CHUN-CHIH HUANG: orange648@gmail.com

Institute of Aeronautics and Astronautics, National Cheng Kung University, No.1, University Road, Tainan 70101, Taiwan